A&A 472, 887–895 (2007)
DOI: 10.1051/0004-6361:20077551

Astronomy & Astrophysics

EK Draconis⋆,⋆⋆

Magnetic activity in the photosphere and chromosphere

S. P. Järvinen[1,2], S. V. Berdyugina[3,4], H. Korhonen[1], I. Ilyin[1], and I. Tuominen[5]

[1] Astrophysikalisches Institut Potsdam, An der Sternwarte 16, 14482 Potsdam, Germany
e-mail: [sjarvinen;hkorhonen]@aip.de
[2] Astronomy Division, PO Box 3000, 90014 University of Oulu, Finland
[3] Institute of Astronomy, ETH Zentrum, 8092, Zürich, Switzerland
e-mail: sveta@astro.phys.ethz.ch
[4] Tuorla Observatory, University of Turku, 21500 Piikkiö, Finland
[5] Observatory, PO Box 14, University of Helsinki, 00014 Helsinki, Finland

Received 27 March 2007 / Accepted 22 June 2007

ABSTRACT

Context. As a young solar analogue, EK Draconis provides an opportunity to study the magnetic activity of the infant Sun.
Aims. We present three new surface temperature maps of EK Draconis and compare them with previous results obtained from long-term photometry. Furthermore, we determined a set of stellar parameters and compared the determined values with the corresponding solar values.
Methods. Atmospheric parameters were determined by comparing observed and synthetic spectra calculated with stellar atmosphere models. Surface temperature maps were obtained using the Occamian approach inversion technique. The differential rotation of EK Dra was estimated using two different methods.
Results. A detailed model atmosphere analysis of high resolution spectra of EK Dra has yielded a self-consistent set of atmospheric parameters: $T_{\rm eff}$ = 5750 K, $\log g$ = 4.5, [M/H] = 0.0, $\xi_{\rm t}$ = 1.6 km s^{-1}. The evolutionary models imply that the star is slightly more massive than the Sun and has an age between 30−50 Myr, which agrees with the determined lithium abundance of $\log N$(Li) = 3.02. Moreover, the atmospheric parameters, as well as the wings of the Ca II 8662 Å, indicate that the photosphere of EK Dra is very similar to the one of the present Sun, while their chromospheres differ. There also seems to be a correlation between magnetic features seen in the photosphere and chromosphere. The temperature images reveal spots of only 500 K cooler than the quiet photosphere. The mean spot latitude varies with time. The obtained differential rotation is very small, but the sign of it supports solar type differential rotation on EK Dra.

Key words. stars: imaging – stars: activity – stars: starspots – stars: individual: EK Dra

1. Introduction

Solar analogues of various ages, and therefore also various levels of activity, provide an opportunity to examine the past and future evolution of the Sun without significant or total recourse to stellar models. Because of nuclear reactions in its core, the Sun is a slowly evolving variable star that has undergone a ∼40% increase in luminosity over the past 4.5 Gyr, as predicted by the standard solar evolution model (e.g., Girardi et al. 2000). On much shorter time scales, the Sun is a magnetically variable star with an ∼11 yr sunspot and activity cycle, and a ∼22 yr magnetic cycle. Although the magnetic activity of the present Sun is relatively weak compared to other active stars, the magnetically induced phenomena have important effects on the Earth and the Solar system. One of the fundamental questions is whether the Sun has always been a relatively inactive star or has it experienced some periods of stronger magnetic activity. The observations show that Zero-Age Main Sequence (ZAMS) solar-type stars can rotate over 10 times more rapidly than today's Sun (Güdel et al. 1997). As a consequence of this, young solar-type stars, including the young Sun, have vigorous magnetic dynamos and correspondingly strong high-energy emissions. Studies of solar-type stars with different ages show that the Sun loses angular momentum with time due to magnetic braking (e.g., Skumanich 1972; Simon et al. 1985).

In the study of patterns of variation in the Sun-like stars, Radick et al. (1998) conclude that more active stars tend to become fainter during their activity cycle as their Ca II H & K emission increases, while the older, less active stars, including the Sun, tend to become brighter. This implies a shift from the spot-dominated to faculae-dominated activity. Moreover, the young, more active stars seem to have stronger short-term and weaker long-term variation patterns, opposite to the solar case, where the long-term variations are the most pronounced. However, the same study reveals, that when looking at only the short-term (i.e., night to night) variations in the chromospheric emission

⋆ Based on observations made with the Nordic Optical Telescope, operated on the island of La Palma jointly by Denmark, Finland, Iceland, Norway, and Sweden, in the Spanish Observatorio del Roque de los Muchachos of the Instituto de Astrofisica de Canarias.
⋆⋆ Table 1 and Figs. 7 and 8 are only available in electronic form at http://www.aanda.org

and brightness, all Sun-like stars, independent of age, become fainter as their chromospheric emission increases. For the Sun, this is due to active regions: the dark sunspots and the bright emission plages are spatially colocated. A similar short-term trend in all Sun-like stars may indicate that their surface magnetic regions tend to be organised broadly in a similar way to the Sun's.

The average level of chromospheric activity and rotation both change on an evolutionary time scale (see, e.g., Wilson 1963, 1966; Kraft 1967; Skumanich 1972). The young Sun should have had a high S-index (the observable quantity used in the Mount Wilson H & K survey to measure chromospheric emission), rapid rotation, no Maunder minimum phase, and only a rare occurrence of a smooth cycle in the chromospheric emission (Baliunas et al. 1995). EK Dra (HD 129333) is not a solar twin, but the properties of the star do not deviate much from those of the Sun, allowing us to consider it as a young solar analogue. And it is still the best proxy for the young Sun we have.

In a solely photometric study Järvinen et al. (2005) determined the time dependence of spot phases on EK Dra using 21 years of photometric observations. Combined with the Sonneberg Sky-Patrol plate results (Fröhlich et al. 2002), their analysis revealed that the total spot area varies on a time scale longer than 45 years with a periodic variation of about 10.5 years. Also, spots were found to group around two active longitudes separated on average by 180° and migrating within the 10.5-yr period.

Strassmeier & Rice (1998) carried out the first Doppler imaging analysis of EK Dra, using observations from March 1995, and found a dominating cool (ΔT = 1200 K) spot located at a latitude of ≈70–80°, thus, far in excess of where our Sun shows spots. Moreover, they also recovered mid-latitude spots, which were only about 400 K cooler than the photosphere. According to the results of Strassmeier & Rice (1998), EK Dra still represents the best stellar approximation of the young solar atmosphere. However, the binary nature of EK Dra reported by König et al. (2005) makes it differ from the young – and present – Sun. The low-mass (0.5 ± 0.1 $M_\odot$) companion of EK Dra orbits it in a highly eccentric (e = 0.82 ± 0.03) orbit, which has a semi-major axis of 14 ± 0.5 AU. The orbital period is 45 ± 5 years, and the minimum distance at the periastron is 2.2 AU (König et al. 2005). It is thus unlikely that this companion has any short-term influence on the magnetic activity of EK Dra and, as such, on the analysis presented in this paper.

We present here new surface maps of EK Dra aiming to study the spot evolution and confirm earlier photometric results. The observations and data reduction are described in Sect. 2 and determinations of stellar parameters in Sect. 3. The line profiles and inversion technique, as well as the resulting temperature maps, are discussed in Sect. 4. The results are discussed in Sect. 5, and finally we summarise our findings in Sect. 6.

2. Observations and data reduction

The spectroscopic observations of EK Dra were carried out during three observing runs – July/August 2001, February/March 2002, and August 2002 – with the Nordic Optical Telescope (NOT, La Palma) using the SOFIN échelle spectrograph, which in 2002 was equipped with a new CCD. The data were acquired with the 2nd camera, which provided 33 useful orders in a spectral range of 3930−9040 Å.

With the old CCD and the slit width of 81 μm, the 2001 observations have resolution ($\lambda/\Delta\lambda$) of 77 000 and the spectra are centred at 6439 Å. With the new CCD during the two 2002 runs, the slit width was 65 μm and 64 μm, giving the resolution of 76 000 and 77 000, respectively. During the first 2002 run the spectra were centred at 6427 Å and during the later run again at 6439 Å. More information is presented in Table 1, which is only available online.

All the NOT spectra were reduced with the 4A software package (Ilyin 2000). The reduction included bias subtraction, estimate of the variance of the flux, master flat-field correction, scattered light subtraction with the aid of 2D-smoothing splines, spectral order definition, and weighted integration of the flux with cosmic spike elimination. The wavelength calibration was obtained using Th-Ar comparison spectra.

In 2005, EK Dra was also observed at the Canada-France-Hawaii telescope (CFHT) with the ESPaDOnS spectrograph as a part of a spectro-polarimetric survey of cool active stars by Berdyugina et al. (2005), who reported the first direct detection of a magnetic field on EK Dra. The spectrum covered the whole optical wavelength range with the resolution of 67 000. Here, we analyse only the Li 6707 Å line from this spectrum.

3. Stellar parameters

3.1. Atmospheric parameters

A list of atomic line parameters for a given wavelength region was obtained from the Vienna Atomic Line Database (VALD) for lines having a central depth of 1% or more (e.g., Piskunov et al. 1995; Kupka et al. 1999). Stellar model atmospheres used are from Kurucz (1993).

To obtain a self-consistent set of parameters, we used the procedure described by Berdyugina et al. (1998).

1. Assuming first an appropriate pair of $T_{\rm eff}$ and $\log g$, we analysed neutral metal lines to produce a set of curves (loci of constant equivalent width) on a diagram of metal abundance, [M/H], as a function of microturbulence, $\xi_{\rm t}$. The curves intersect in a narrow region, which provides the initial estimate for [M/H] and $\xi_{\rm t}$ (Fig. 1a). The "loci of constant equivalent width" in the sense of the synthetic spectrum calculations means the best fit to the observed spectrum.
2. Using the initial estimates of [M/H] and $\xi_{\rm t}$, we analysed both neutral and ionised metal lines to produce a set of curves on a diagram of $T_{\rm eff}$ versus $\log g$. Since lines of ionised metals are sensitive to both parameters and lines of neutral metals are mostly sensitive to the temperature, the intersection region gives an initial estimate of a pair of $T_{\rm eff}$ and $\log g$ values (Fig. 1b).
3. The previous two stages were iterated until a self-consistent set of parameters was obtained.

The results are given in Table 2, where for comparison values determined by Strassmeier & Rice (1998), referred to as S&R, and König et al. (2005), referred to as KGWH, are shown. The parameters are very similar to the present solar values, implying that, since EK Dra is much younger than the Sun, the stars should have different masses.

3.2. Mass, age, and lithium abundance

The stellar mass can be estimated from the ($T_{\rm eff}$, $L/L_\odot$)-diagram (Fig. 2), where EK Dra is placed slightly above the 1 $M_\odot$ evolutionary track (Granzer et al. 2000), suggesting a mass of 1.02 $M_\odot$. The $T_{\rm eff}$ value was determined as described in Sect. 3.1.

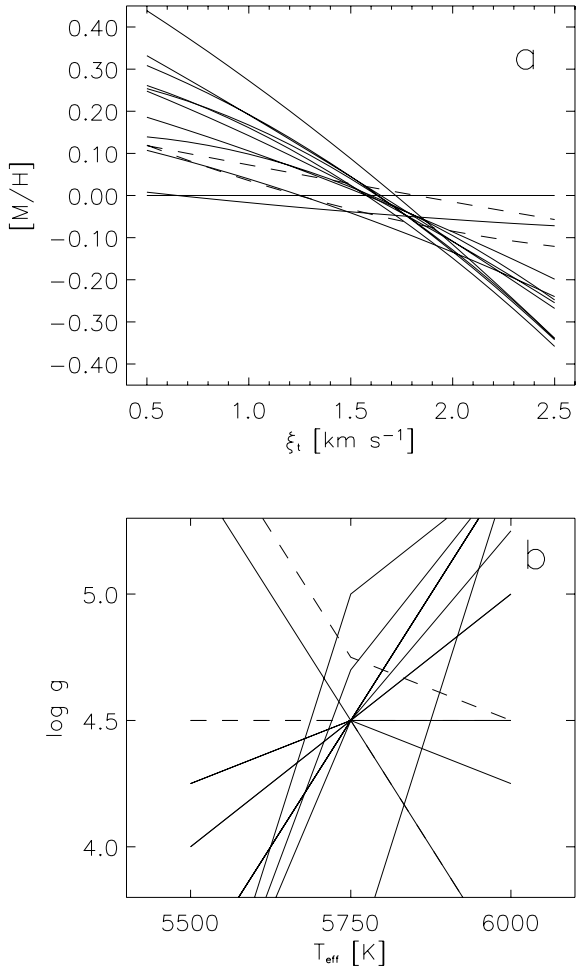

Fig. 1. a) and **b)** Diagrams for self-consistent determination of the atmospheric parameters of EK Dra: **a)** metallicity [M/H] and microturbulence ξ_t, **b)** effective temperature $T_{\rm eff}$, and surface gravity $\log g$. Solid curves represent iron lines, and dashed ones represent other metals.

Table 2. Atmospheric parameters of EK Dra.

Parameter	Value	S&R	KGWH[a]
$T_{\rm eff}$, K	5750 ± 50	5870 ± 50	5700 ± 70
$\log g$	4.5 ± 0.1	4.5	4.37 ± 0.10
[M/H]	0.00 ± 0.05	0.0	–0.16
ξ_t, km s^{-1}	1.6 ± 0.1	2.0	–
ζ_t, km s^{-1}	3.0	4.0	–
$v \sin i$, km s^{-1}	17	17.3 ± 0.4	16.5 ± 1.0
Inclination, i	60°	60°	–
$\log N$(Li)	3.02 ± 0.02	–	3.30 ± 0.05

[a] The [M/H] value is [Fe/H].

Here, the question arises whether a persistent spot has any influence on the spectroscopic analysis. This was tested for EK Dra by König et al. (2005) using H_α and H_β line profiles. They assumed a spot coverage of 1/4 of the visible surface and a spot temperature of 4500 K. This spot configuration did not change the results significantly since continuum of the spot is only about 10% of the continuum level of the surrounding stellar surface. Also, since a spot is much cooler than the photosphere, its total contribution to the light emitted from the star is very small. The humps and line centre shifts, which are typical indicators of the presence of spots on the stellar surface, are not seen by eye

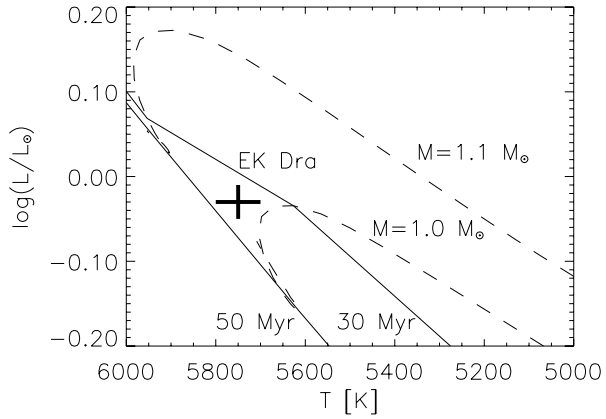

Fig. 2. The position of EK Dra in the ($T_{\rm eff}$, $L/L_\odot$)-diagram. The evolutionary tracks for masses 1.0 and 1.1 $M_\odot$ (dashed lines) and isochrones for 30 Myr and 50 Myr (solid lines) are from Granzer et al. (2000).

in observed line profiles (see, for example Fig. 6). However, in the stellar parameter determination, in order to minimise these effects, we used the spectrum averaged over all phases. This way the used spectrum is dominated by the photosphere. The luminosity $L/L_\odot$ was determined from the maximum V magnitude of EK Dra. The 21 years of photometric observations show a decreasing trend in the brightness. The older measurements from Sonneberg Sky-Patrol plates (Fröhlich et al. 2002) show that EK Dra was even brighter in the past. Therefore, for determining the unspotted V magnitude, the maximum V magnitude of each individual subset (from Järvinen et al. 2005) was plotted against the amplitude of the subset. From this plot the maximum V magnitude at the zero amplitude was determined, i.e., with no spots on the surface. The investigation yielded an unspotted magnitude of $V = 7\overset{\rm m}{.}48$. The absolute magnitude $M_{\rm V} = 4\overset{\rm m}{.}80$ was calculated using the *Hipparcos* distance 33.94 ± 0.72 pc, applying the bolometric correction (Flower 1996) and correcting for the interstellar extinction (Schlegel et al. 1998).

Our estimate of the mass is in good agreement with an earlier result by Dorren & Guinan (1994) and is also within the error bar of the value determined in a kinematic study by König et al. (2005), who reported the mass of 0.9 ± 0.1 $M_\odot$.

The isochrones (Granzer et al. 2000) shown in Fig. 2 suggest that EK Dra has an age between 30 Myr and 50 Myr. This is clearly less than the age of the Pleiades, which has values ranging from ~80 Myr (Mermilliod 1981) to 125 Myr (see, e.g., Ferrario et al. 2005). However, the age estimate we get agrees with EK Dra belonging to the Local Association (Montes et al. 2001), since members of this supercluster are estimated to span the relatively broad range of ages from a few Myr to a few hundred Myr (e.g., Eggen 1992; Asiain et al. 1999).

From the CFHT spectrum, we determined the Li I line equivalent width of 195 mÅ. This agrees with the value of 198 mÅ reported by Montes et al. (2001). The value is between the upper limit values of equivalent widths measured for stars in the Pleiades and IC 2602. This lithium abundance supports our finding that EK Dra is significantly younger than the Pleiades open cluster. For determining the lithium abundance, we performed a spectral synthesis analysis, including both atomic and CN line blends. The best fit was achieved with the lithium abundance $\log N(\rm Li) = 3.02$ in the scale $\log N(\rm H) = 12$ (Fig. 3). This is smaller than the value reported by König et al. (2006), who determined $\log N(\rm Li) = 3.30 \pm 0.05$.

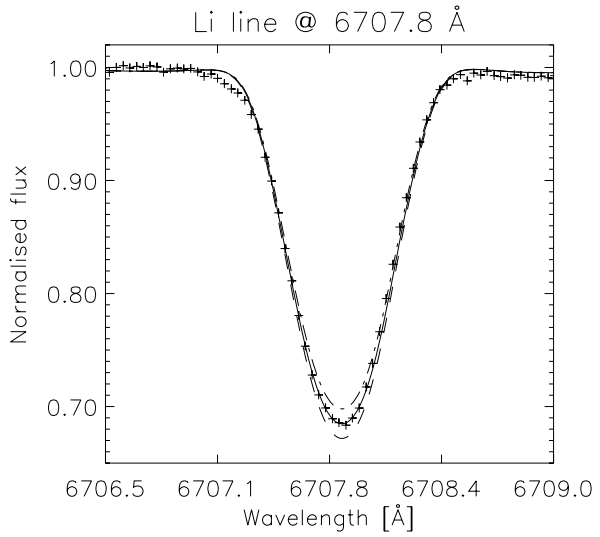

Fig. 3. The observed lithium absorption line at 6707.8 Å denoted with + symbols. The solid line represents the best fit to the observations with lithium abundance log N(Li) = 3.02. For comparison, the dashed line denotes a fit with 0.05 dex higher, and the dash-dot line a fit with 0.05 dex lower lithium abundance.

4. Doppler imaging

4.1. Line profiles and inversions

Four atomic lines were selected for Doppler imaging: Fe I 6419.95 Å, Fe I 6421.35 Å, Fe I 6430.80 Å, and Ca I 6439.08 Å. Local line profiles were calculated with the code by Berdyugina (1991), which includes calculations of opacities in the continuum and in atomic and molecular lines, although molecular lines were omitted here, since they do not contribute to the spectrum of EK Dra. As mentioned in Sect. 3.1, atomic line parameters were obtained from VALD. The local line profiles were calculated for 20 values of $\mu = \cos\theta$ from the disk centre to the limb. The spectra were calculated from temperatures ranging from 4000 K to 6500 K in steps of 250 K.

The Occamian approach was used for inversions of the observed line profiles into stellar images (Berdyugina 1998). A $6^\circ \times 6^\circ$ grid on the stellar surface was used for integrating local line profiles into normalised flux profiles. With a set of stellar atmosphere models, the stellar image is considered as the distribution of effective temperature across the stellar surface, as is usually done in surface imaging. The adopted stellar parameters are given in Table 2.

The phases of the observations were calculated using the ephemeris by Järvinen et al. (2005):

$$T = 2\,445\,781.859 + 2\overset{\mathrm{d}}{.}606\,E. \quad (1)$$

4.2. Temperature maps

The surface temperature maps of EK Dra for the years 2001.56, 2002.16, and 2002.65 are shown in Fig. 4. They show both high- and low-latitude spots, but only in the first map is a very high-latitude spot, i.e., partly above 60°, present. The recovered spots are at most 500 K cooler than the unspotted stellar surface, while the hot regions are hotter by almost the same amount. The poor contrast in temperature is most likely due to the insufficient spectral resolution. All the three maps show spots around longitude $l = 20^\circ$, but the high-latitude extension of this spot diminishes with time. Both maps from 2002 clearly show an active region 180° away from the $l = 20^\circ$ spot.

The longitudes of the spectroscopic observations are shown at the bottom of the Mercator projections of the temperature maps (Fig. 5, top panel), in the area from which we have no information due to the inclination of the star. The fits to the observed spectra are shown in Fig. 6 for the 2001.56 data set and online in Figs. 7 and 8 for the 2002.16 and 2002.65 data sets, respectively, for all the four lines used in the inversions.

The Doppler image of EK Dra obtained by Strassmeier & Rice (1998) from 12 spectral lines revealed spot temperatures of 1200 K and 400 K cooler than the photosphere. On the other hand, the photometric study of Alekseev (2003) indicates that spots may even be 2200 K cooler than the photosphere, a result that is quite similar to the one by O'Neal et al. (2004) based on TiO-band observations. Our maps (Fig. 4) show a temperature difference between the photosphere and the spots of the order of only a few hundred Kelvins, which is similar to the one recovered by Strassmeier & Rice (1998) for most of the spots, excluding the dominating high-latitude feature. Berdyugina (2005) has suggested that the low-temperature contrast of spots and small spot filling factors can be due to a decrease in individual spot sizes and, thus, an increase in the relative contribution from the spot penumbra. The spot contrast we obtained corresponds to the temperature contrast of the sunspot penumbra.

5. Discussion

5.1. Spot latitudes

The top panel of Fig. 9 shows the latitudinal spot distributions at different times. For all the maps, one temperature value (5600 K) was chosen to represent a limit between the spots and unspotted photosphere. This limit is rather high due to a very narrow temperature range in the 2002.16 map. When looking at the whole latitude range, one can see that high-latitude spots disappear in the 2002.16 map and also that the peak at high latitudes moves towards lower latitudes between 2001.56 and 2002.16. In the 2002.65 map higher latitudes are again covered with spots. The low-latitude spots seem to prefer approximately the same latitude range, peaking at +5°, but the fractional coverage varies with time, being at the minimum in 2002.65. However, the mean spot latitude changes only slightly, shifting first clearly towards lower latitudes, and then somewhat back towards higher latitudes.

We were also interested in seeing whether the spots have different latitudes around the opposite active longitudes derived by Järvinen et al. (2005). According to the traced active longitudes, the first active longitude is centred at the longitude $l = 72^\circ$ for the 2001.56 map, $l = 42^\circ$ for the 2002.16 map and $l = 60^\circ$ for the 2002.65 map, and the second active longitude is centred 180° apart from the first one. When looking at the latitude range around the first active longitude (Fig. 9, middle panel), one can notice that the high-latitude (+70°) spot was rather prominent in 2001.56. Half a year later, in 2002.16, the spot concentration moved towards lower latitudes, and there were no spots at high latitudes. In 2002.65 all the spots around the first active longitude were concentrated only at low latitudes and were distributed almost evenly around the equator. The latitude range around the second active longitude was generally dominated by low-latitude spots. In 2001.56 the major spot concentration was around the equator, although a tip of the extension of the high-latitude feature from the opposite active longitude was also present. In 2002.16, the spot coverage had two peaks at

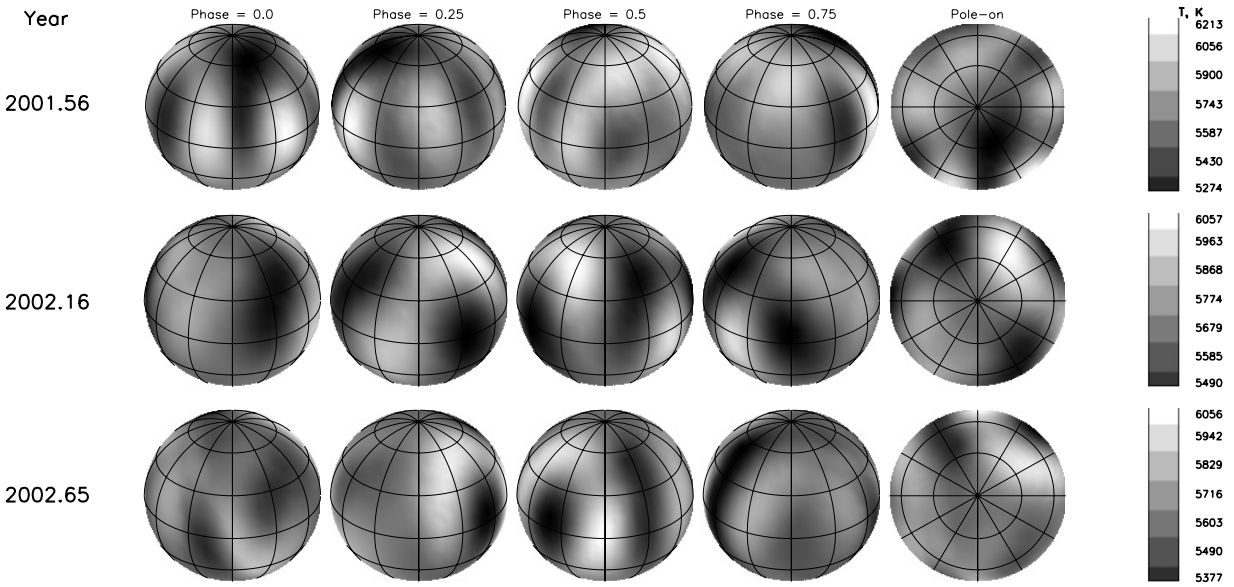

Fig. 4. The surface temperature maps of EK Dra for three seasons obtained with the Occamian approach. Note the changing temperature scale.

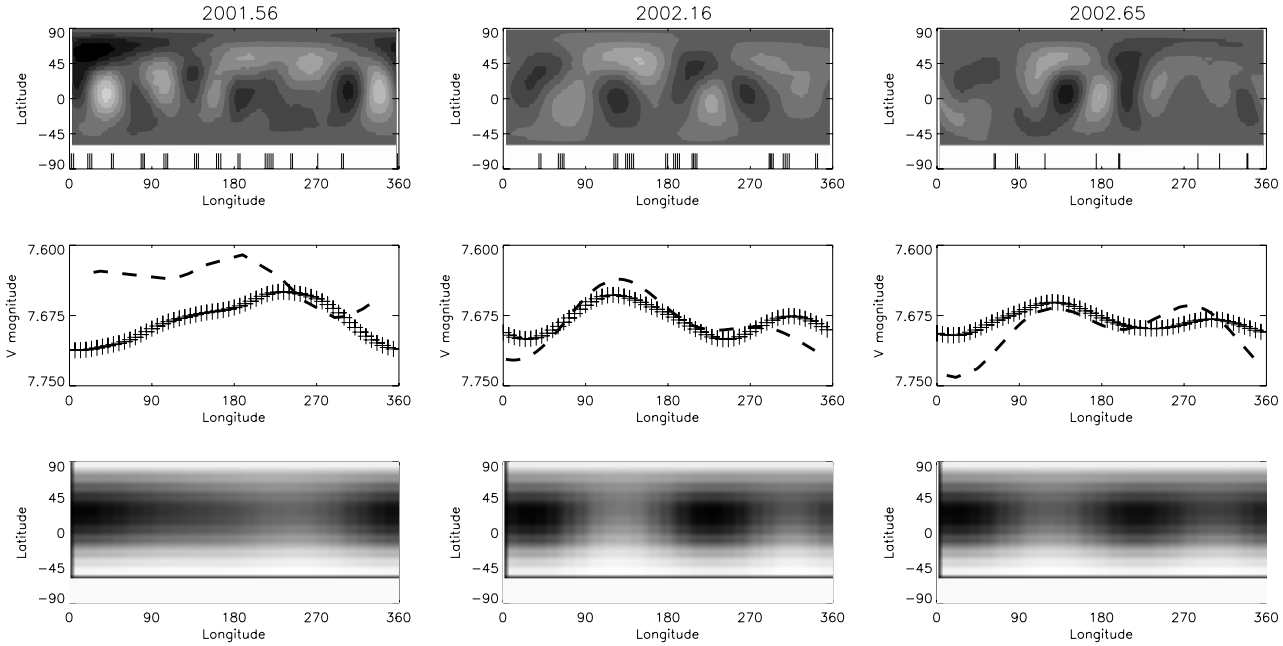

Fig. 5. *Top panels*: the surface temperature maps from Fig. 4 shown in the Mercator projection. The phases of the spectroscopic observations are shown with vertical dashes at the bottom in the area from which we have no information due to the inclination of the star. *Middle panels*: light curves calculated from the temperature maps (crosses). The dashed lines represent the closest photometric observations in time. The light curve for the 2001.56 image was obtained more than 2.5 months earlier than the spectra and has a rather poor phase coverage. The 2002.16 photometry is taken within a month after the spectra, and the one for 2002.65 two months earlier. *Bottom panels*: spot filling factor maps obtained by inversions from the calculated light curves (shown with crosses in the middle panels) as was done previously from real photometric observations by Järvinen et al. (2005). The darker colour corresponds to a higher filling factor.

+10° and +40°. In 2002.65, the mid- and low-latitude fractions were almost equal. To summarise, the mean spot latitude around the first active longitude was shifting towards the equator (by ∼25° within a year) and around the second active longitude towards the visible pole (by ∼15° within the same time interval). Such behaviour was also found on a very active RS CVn-type star HR1099 (Berdyugina & Henry 2007). Moreover, the longitudinal and latitudinal drifts were found to be in correlation with the stellar activity cycle, which was interpreted as a precession of the global stellar magnetic field with respect to the stellar rotational axis. It would be interesting, therefore, to obtain a series of Doppler images of EK Dra at various phases of its activity cycle and investigate this phenomenon in detail.

5.2. Comparison with long-term photometry

The results by Fröhlich et al. (2002) and Järvinen et al. (2005) indicated that the magnitude of EK Dra was decreasing for at least the past 45 years. This implies that a part of the surface is

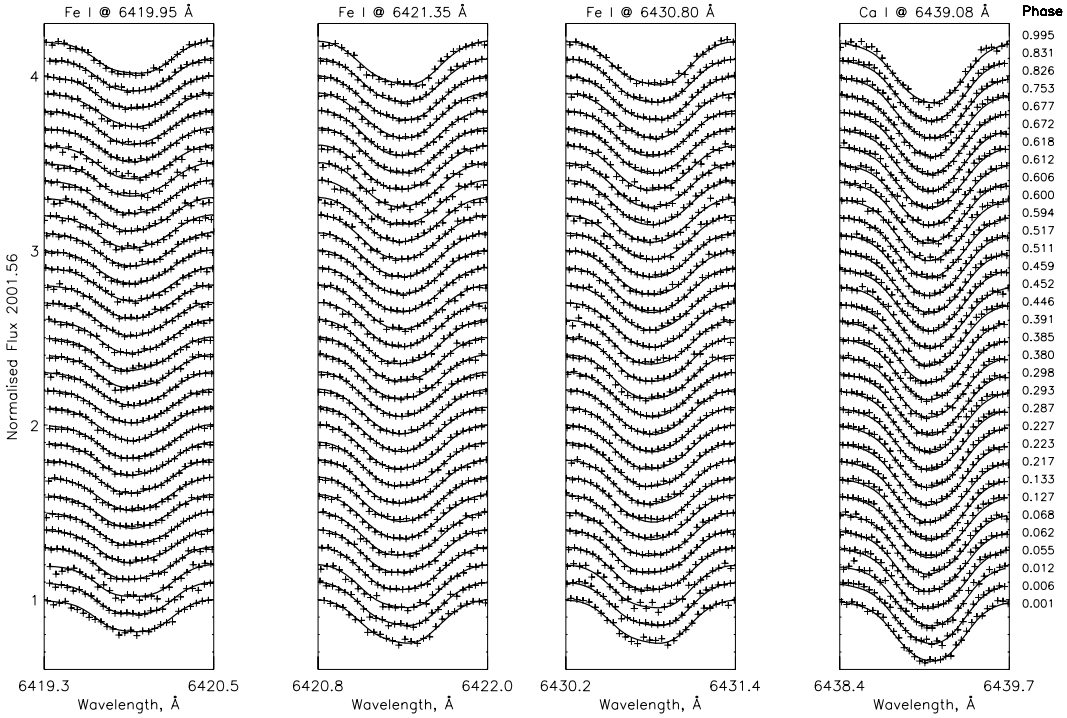

Fig. 6. Calculated (lines) and observed (crosses) spectral lines for the 2001.56 data set.

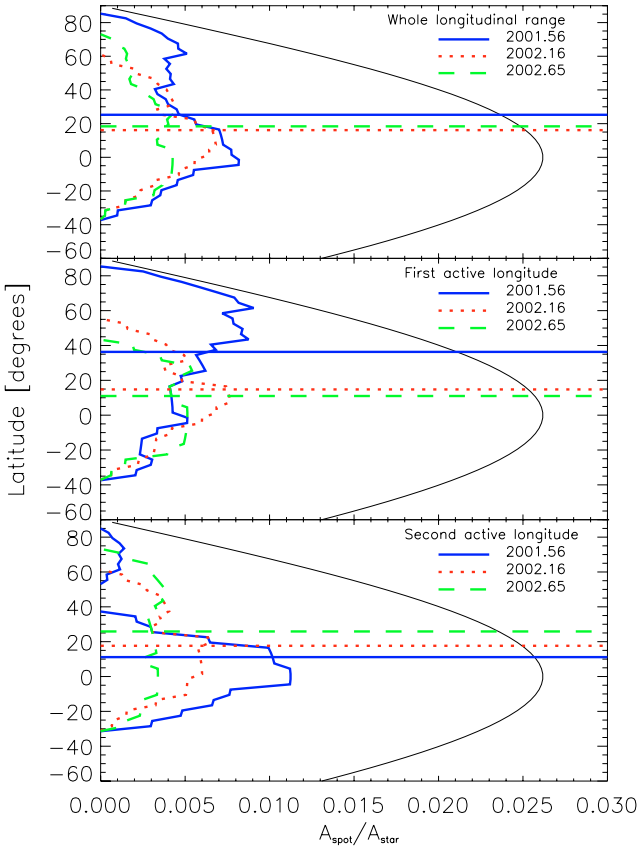

Fig. 9. The latitudinal distribution of the spots recovered in the three surface maps (thick lines). The thin solid curve denotes the fraction of the stellar surface within each latitude, and the horizontal lines mark the mid latitude of the spots. Both active longitudes have a width of 180°. *Top panel*: the whole longitudinal range. *Middle panel*: around the first active longitude. *Bottom panel*: around the second active longitude.

continuously covered with spots. However, seasonal amplitude variations imply that at least some of the spots evolve with time.

In the previous photometric study of EK Dra, we determined the time dependence of spot phases (Järvinen et al. 2005). The results from this study are shown in Fig. 10, where both the primary spots and secondary spots are marked. If it was not possible to determine which spot was the primary, both were denoted with a plus sign. It was concluded that the spots were concentrated on two active longitudes separated by 180° that migrate due to differential rotation. To investigate how the new temperature maps (Fig. 5, top panel) correspond to the long-term activity deduced from the photometry, we synthesised light curves (Fig. 5, middle panel) from them, which were then inverted into spot filling factor maps (Fig. 5, bottom panel), as we had done earlier for real photometric observations. A comparison of the two types of maps indicate that the spot phases in the filling factor maps correspond to the mean phases of either individual spots or groups of spots recovered in the Doppler images.

For comparison, the real photometric observations nearest in time are also plotted in Fig. 5 (middle panel). Unfortunately, in none of the cases were there simultaneous photometric observations. For instance, the photometry was obtained for the first data set more than 2.5 months earlier than the spectra and has a poor phase coverage. However, the real photometry for the two later sets shows rather similar behaviour as compared to the photometry calculated from the maps.

The synthetic light curves clearly show how, in the time interval of about a year, a spot forms at $l = 235°$, while the spot coverage around the phase $l = 20°$ shrinks slightly when the high-latitude extension, seen in the Doppler maps, disappears. The phases of the spots determined from the synthetic light curves (Fig. 10) agree well with the phases determined from the real photometric observations. This supports the idea that the cyclic migration of the spot phases, determined from the photometric inversions, is indeed real.

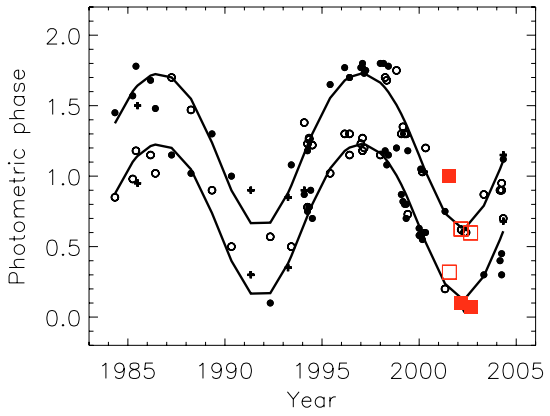

Fig. 10. The time dependence of the phases of the spots on EK Dra adopted from Järvinen et al. (2005). The primary spots are marked with black dots and secondary ones with open circles. If it was not possible to say which spot was the primary, both are denoted with +. The spots are concentrated on two active longitudes (traced by solid lines) that migrate due to differential rotation. The phases of the spots determined from the synthetic light curves (calculated from the surface temperature maps) are marked as follows: primary spots are (red) filled squares and secondary spots are (red) open squares.

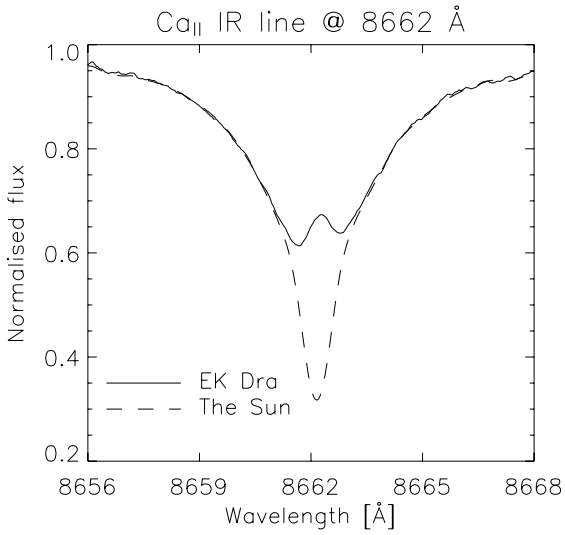

Fig. 11. The average profile of all Ca II IRT-3 lines obtained with the NOT (solid line), together with the rotational broadened observed solar profile from the solar atlas (dashed line).

5.3. The chromospheric activity

In the beginning of 1989, Dempsey et al. (1993) observed Ca II infrared triplet (IRT) lines in 45 stars, including EK Dra. They reported emission reversals in both IRT-1 and IRT-2 lines, but not in the IRT-3 line. Our spectra obtained at the NOT included only the IRT-3 line (8662 Å), and we clearly see an emission reversal in this line, as visualised in Fig. 11. The difference in the emission reversals between our spectra and those by Dempsey et al. (1993) is consistent with the changes in activity level seen in the long-term photometry. In 1989 the star was on average $0\overset{\mathrm{m}}{.}05$ brighter than in 2002, and the amplitude of the light curve was also smaller, implying a lower activity level.

It is remarkable that the rotationally broadened observed solar profile matches the wings of the average Ca II IRT-3 line profile of EK Dra perfectly, which implies that the photospheres of the two stars are very similar, thus confirming the atmospheric parameters we have determined. On the other hand, the emission reversal indicates that the chromospheres are not identical.

For a more detailed analysis of the emission reversal profiles, we subtracted the broadened solar profile from the observed profiles. Figure 12 shows the time variation of the Ca II IRT-3 line emission reversal equivalent width (W_λ), plotted together with the shapes of the synthetic light curves calculated from the temperature maps. During the first observing run, the equivalent width clearly has two peaks, at phases $\varphi = 0.05$ and $\varphi = 0.55$. The first peak corresponds to the high-latitude spot seen in the 2001.56 temperature map (see Fig. 5), while the second peak is at a slightly later phase than the spot concentration at the lower latitudes. During the second run, peaks are at $\varphi = 0.15$ and at $\varphi = 0.6$–0.8. Both peaks correspond to the mid-latitude spots in the 2002.16 map, although not so clearly for the second peak due to sparse observations. The last data set does not have enough measurements for any clear conclusions, but there may be a peak between $\varphi = 0.9$–0.15, which could correspond to the mid-latitude spot at $\sim\varphi = 0.1$ in the 2002.65 map.

Thus, it appears that the equivalent width of the Ca II IRT-3 line is in a maximum when the light curve has a minimum, and vice versa, which implies that the spots in the photosphere are cospatial with the active regions in the chromosphere, the result being similar to other active stars (e.g., Berdyugina et al. 1999). Also, since the emission reversal is detected in all observed spectra and measured W_λ never goes to zero, this indicates that there is always some fraction of the chromosphere covered with plages, as well as some fraction of the photosphere covered with spots.

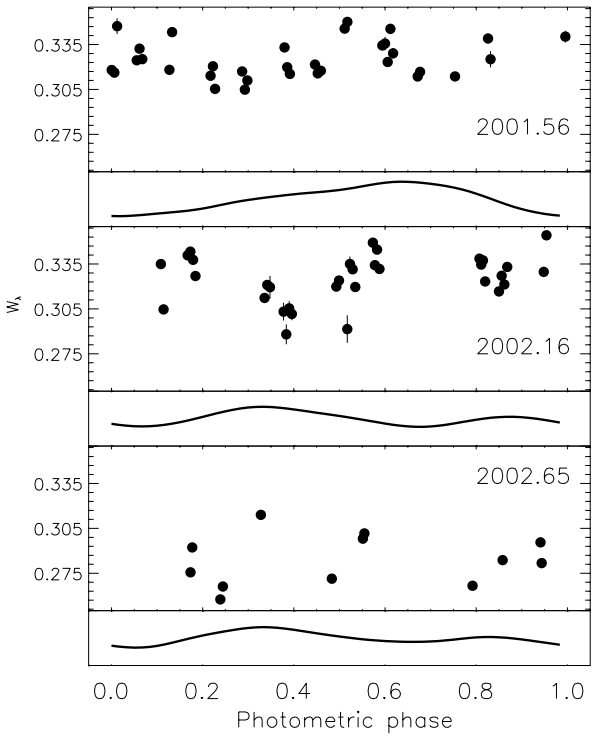

Fig. 12. Time variation of the Ca II IRT-3 line emission reversal equivalent width (W_λ) marked as dots. For comparison under each data set the shape of light curve calculated from the temperature maps is shown with a solid line.

5.4. Differential rotation estimation

The surface differential rotation on EK Dra was estimated by employing two different approaches. The first approach is based on mean spot latitudes derived from the Doppler images presented in the current paper and the one by Strassmeier & Rice (1998), obtained for the year 1995. In the 1995 map the mean spot latitude is 45°. The rotation periods at the times of the maps were determined based on the migration pattern of the active longitudes presented in Fig. 10. The differential rotation law used is

$$\Omega(\psi) = \Omega_0 + \beta \sin^2 \psi, \quad (2)$$

where $\Omega(\psi)$ is the angular velocity at latitude ψ, Ω_0 the equatorial angular velocity, and β the differential rotation $\Omega_0 - \Omega_{\rm pole}$. The parameter α is defined as

$$\alpha = \frac{-\beta}{\Omega_0}.$$

The derived mean latitude and rotation periods allow us to plot Ω as a function of $\sin^2 \psi$ (Fig. 13), giving $\Omega_0 = 138.188 \pm 0.001$ degrees per day, $\beta = -0.126 \pm 0.002$ degrees per day, and $\alpha = 0.00091 \pm 0.00001$. The negative sign of β indicates a solar type differential rotation, i.e., more rapid rotation at the equator.

The second approach is based on the cross-correlation of the two temperature maps obtained for the year 2002. They are separated by half a year and have similar spot configurations. As described in Korhonen et al. (2000), β in Eq. (2) can be determined from the measurements of the longitudinal shifts of the spots at different latitudes. The lowest latitude that had spots, $\psi_* = 1.5°$ was chosen as the reference latitude. For calculating the shift at each latitude, the shift at the reference latitude was first subtracted. Then the phase of the maximum cross-correlation function was determined by fitting a second-degree polynomial to the cross-correlation function and calculating the phase of the maximum from the fit. After this, the shift was converted to degrees per day. The β value was determined by using a linear fit to the residual shifts in degrees per day plotted against the $\sin^2(\psi) - \sin^2(\psi_*)$. This investigation results in $\beta = -0.15 \pm 0.02$, which is within the errors the same as the value obtained using the latitudes from the Doppler images and the rotation period from the active longitudes, thus supporting the result from the first approach.

Our estimate of the possible range of the differential rotation is much smaller than predicted for a late type dwarf with the period of EK Dra by the models of Kitchatinov & Rüdiger (1999). It is also too small to match an empirical relation between the differential rotation and the temperature and rotation by Barnes et al. (2005).

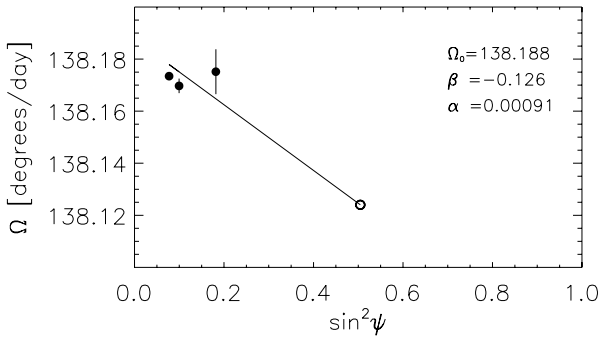

Fig. 13. A plot for determining the differential rotation parameters. The filled circles represent Ω and $\sin^2 \psi$ values determined from the maps in the present paper, while the open circle represents corresponding values from the map by Strassmeier & Rice (1998).

6. Summary

From the spectroscopic study of EK Dra, the following results have been obtained:

1. A detailed model atmosphere analysis of the high-resolution spectra of EK Dra yielded a self-consistent set of atmospheric parameters: $T_{\rm eff} = 5750 \pm 50$ K, $\log g = 4.5 \pm 0.1$, [M/H] $= 0.00 \pm 0.05$, $\xi_{\rm t} = 1.6 \pm 0.1$ km s^{-1}, $\log N({\rm Li}) = 3.02 \pm 0.02$.
2. Based on the evolutionary tracks by Granzer et al. (2000), EK Dra appears slightly more massive than the Sun ($\sim$1.02 $M_\odot$) and has an age of 30−50 Myr. The lithium abundance of the star supports the younger age than for Pleiades.
3. Excellent correspondence between the EK Dra Ca II IRT-3 line and the rotationally broadened solar profile in the line wings implies that both stars have similar photospheres, thus supporting the determined atmosphere parameters. However, an emission reversal detected in the Ca II IRT-3 line implies that the chromosphere of EK Dra is more active that the Sun's.
4. The three temperature maps for the years 2001 and 2002 obtained by inversions of atomic line profiles show both high- and low-latitude spots about 500 K cooler than the quiet photosphere. The accuracy of the spot temperature is apparently limited by the spectral resolution.
5. The spot phases determined from the synthetic light curves (calculated from the temperature maps) are in a good agreement with the phases determined from the quasi-simultaneous photometry, thus supporting the previous analysis of stellar light curves, which revealed active longitudes and their cyclic migration.
6. The mean spot latitude (over the entire longitude range) shifted towards the equator within a year by $\sim$10°. However, spots around one active longitude moved equatorward by $\sim$25° and around the other active longitude poleward by $\sim$15°.
7. The equivalent width of the emission in the Ca II IRT-3 line seems to increase, while the light curve is at the minimum, implying a spatially correlated photospheric and chromospheric activity on EK Dra.
8. An estimate of the differential rotation is unexpectedly low as compared with both the theoretical predictions and the empirical relations. However, it indicates a solar-type differential rotation on EK Dra, i.e., with the equator rotating more rapidly than the poles.

Acknowledgements. S.P.J. & H.K. acknowledge the support by the Deutsche Forschungsgemeinschaft, grant KO 2320/1-2. S.P.J. also acknowledges the support by Väisälä Foundation, Finland. S.V.B. acknowledges the EURYI Award from the ESF and SNF grants.

References

Alekseev, I. Yu. 2003, ARep, 47, 430
Asiain, R., Figueras, F., Torra, J., & Chen, B. 1999, A&A, 341, 427
Baliunas, S. L., Donahue, R. A., Soon, W. H., et al. 1995, ApJ, 438, 269
Barnes, J. R., Collier Cameron, A., Donati, J.-F., et al. 2005, MNRAS, 357, L1
Berdyugina, S. V. 1991, Izv. Krymsk. Astrofiz. Obs., 83, 102
Berdyugina, S. V. 1998, A&A, 338, 97
Berdyugina, S. V. 2005, Liv. Rev. Sol. Phys., 2, 8
Berdyugina, S. V., & Henry, G. W. 2007, ApJ, 659, L157

Berdyugina, S. V., Jankov, S., Ilyin, I., Tuominen, I., & Fekel, F. C. 1998, A&A, 334, 863
Berdyugina, S. V., Ilyin, I., & Tuominen, I. 1999, A&A, 349, 863
Berdyugina, S. V., Petit, P., Fluri, D. M., Afram, N., & Arnaud, J. 2006, in Solar Polarization Workshop 4, ed. R. Casini, & B. Lites, ASP Conf. Ser., 358, 381
Dempsey, R. C., Bopp, B. W., Henry, G. W., & Hall, D. S. 1993, ApJS, 86, 293
Dorren, J. D., & Guinan, E. F. 1994, ApJ, 428, 805
Eggen, O. J. 1992, AJ, 104, 1482
Ferrario, L., Wickramasinghe, D., Liebert, J., & Williams, K. A. 2005, MNRAS, 361, 1131
Flower, P. J. 1996, ApJ, 469, 355
Fröhlich, H.-E., Tschäpe, R., Rüdiger, G., & Strassmeier, K. G. 2002, A&A, 391, 659
Girardi, L., Bressan, A., Bertelli, G., & Chiosi, C. 2000, A&AS, 141, 371
Granzer, Th., Schüssler, M., Caligari, P., & Strassmeier, K. G. 2000, A&A, 355, 1087
Güdel, M., Guinan, E. F., & Skinner, S. L. 1997, ApJ, 483, 947
Ilyin, I. 2000, Ph.D. Thesis, University of Oulu, Finland
Järvinen, S. P., Berdyugina, S. V., & Strassmeier, K. G. 2005, A&A, 440, 735
Kitchatinov, L. L., & Rüdiger, G. 1999, A&A, 344, 911
König, B., Guenther, E. W., Woitas, J., & Hatzes, A. P. 2005, A&A, 435, 215
König, B., Guenther, E. W., Esposito, M., & Hatzes, A. P. 2006, MNRAS, 365, 1050
Korhonen, H., Berdyugina, S. V., Hackman, T., Strassmeier, K. G., & Tuominen, I. 2000, A&A, 360, 1067
Kraft, R. P. 1967, ApJ, 150, 551
Kupka, F., Piskunov, N. E., Ryabchikova, T. A., Stempels, H. C., & Weiss, W. W. 1999, A&AS, 138, 119
Kurucz, R. L. 1993, Kurucz CD, No. 13
Mermilliod, J. C. 1981, A&A, 97, 235
Montes, D., López-Santiago, J., Fernández-Figueroa, M. J., & Gálvez, M. C. 2001, A&A, 379, 976
O'Neal, D., Neff, J. E., Saar, S. H., & Cuntz, M. 2004, AJ, 128, 1082
Piskunov, N. E., Kupka, F., Ryabchikova, T. A., Weiss, W. W., & Jeffery, C. S. 1995, A&AS, 112, 525
Radick, R. R., Lockwood, G. W., Skiff, B. A., & Baliunas, S. L. 1998, ApJS, 118, 239
Simon, T., Herbig, G., & Boesgaard, A. M. 1985, ApJ, 293, 551
Schlegel, D. J., Finkbeiner, D. P., & Davis, M. 1998, ApJ, 500, 525
Skumanich, A. 1972, ApJ, 171, 565
Strassmeier, K. G., & Rice, J. B. 1998, A&A, 330, 685
Wilson, O. C. 1963, ApJ, 138, 832
Wilson, O. C. 1966, ApJ, 144, 695

Online Material

Table 1. The spectral observations of EK Dra.

HJD 2450000+	Day	Phase	S/N	Exp. t min	HJD 2450000+	Day	Phase	S/N	Exp. t min
	2001.56				2328.5984990	23/02/2002	0.179	152	20
2120.3987720	29/07/2001	0.287	175	20	2328.6121870	23/02/2002	0.184	142	15
2120.4146610	29/07/2001	0.293	211	20	2329.6258920	24/02/2002	0.573	103	15
2120.4288030	29/07/2001	0.298	181	15	2329.6378240	24/02/2002	0.578	104	15
2121.4021540	30/07/2001	0.672	183	17	2329.6499830	24/02/2002	0.583	137	16
2121.4159430	30/07/2001	0.677	174	17	2329.6638790	24/02/2002	0.588	148	20
2122.4025850	31/07/2001	0.055	161	20	2330.6027570	25/02/2002	0.948	179	20
2122.4184630	31/07/2001	0.062	138	20	2330.6181560	25/02/2002	0.954	197	20
2122.4343350	31/07/2001	0.068	121	20	2331.6132130	26/02/2002	0.336	117	20
2123.4212100	01/08/2001	0.446	122	20	2331.6286220	26/02/2002	0.342	93	20
2123.4370920	01/08/2001	0.453	84	20	2331.6440300	26/02/2002	0.348	55	20
2123.4547670	01/08/2001	0.459	126	25	2331.7063070	26/02/2002	0.372	35	20
2124.4102500	02/08/2001	0.826	186	20	2331.7217160	26/02/2002	0.378	50	20
2124.4245770	02/08/2001	0.831	146	17	2331.7371230	26/02/2002	0.384	52	20
2125.4305090	03/08/2001	0.217	157	20	2331.7536810	26/02/2002	0.390	71	20
2125.4441470	03/08/2001	0.223	147	15	2331.7690890	26/02/2002	0.396	69	20
2125.4561510	03/08/2001	0.227	148	15	2333.6265270	28/02/2002	0.108	208	20
2126.4121150	04/08/2001	0.594	96	20	2333.6419330	28/02/2002	0.114	193	20
2126.4274800	04/08/2001	0.600	82	20	2334.6291160	01/03/2002	0.493	153	20
2126.4428350	04/08/2001	0.606	89	20	2334.6445240	01/03/2002	0.499	100	20
2126.4581960	04/08/2001	0.612	87	20	2334.6917530	01/03/2002	0.517	36	20
2126.4735670	04/08/2001	0.618	74	20	2334.7071620	01/03/2002	0.523	59	20
2127.4581570	05/08/2001	0.995	89	15	2334.7225730	01/03/2002	0.529	118	20
2127.4714840	05/08/2001	0.001	77	19	2334.7374550	01/03/2002	0.535	186	18
2127.4866270	05/08/2001	0.006	85	20	2335.5586800	02/03/2002	0.850	173	20
2127.5024840	05/08/2001	0.012	57	20	2335.5741160	02/03/2002	0.856	173	20
2128.4590970	06/08/2001	0.380	125	20	2335.5895560	02/03/2002	0.862	171	20
2128.4744680	06/08/2001	0.385	111	20	2335.6060060	02/03/2002	0.868	154	20
2128.4898390	06/08/2001	0.391	116	20		*2002.65*			
2129.4335540	07/08/2001	0.753	123	16	2507.4038300	20/08/2002	0.792	166	20
2130.4073500	08/08/2001	0.127	156	20	2508.3978770	21/08/2002	0.173	167	12
2130.4227200	08/08/2001	0.133	159	20	2508.4077730	21/08/2002	0.177	105	12
2131.4089380	09/08/2001	0.511	154	20	2509.3830290	22/08/2002	0.551	178	12
2131.4242990	09/08/2001	0.517	150	20	2509.3915400	22/08/2002	0.555	185	8
	2002.16				2510.3981930	23/08/2002	0.941	177	10
2327.6294150	22/02/2002	0.807	115	12	2510.4049600	23/08/2002	0.944	119	5
2327.6392790	22/02/2002	0.811	155	12	2511.4060840	24/08/2002	0.328	125	15
2327.6491420	22/02/2002	0.815	132	12	2514.4175660	27/08/2002	0.483	233	20
2327.6617820	22/02/2002	0.820	168	20	2515.3936520	28/08/2002	0.858	208	20
2328.5676690	23/02/2002	0.167	133	20	2516.3862990	29/08/2002	0.239	101	20
2328.5830830	23/02/2002	0.173	149	20	2516.4008840	29/08/2002	0.244	116	18

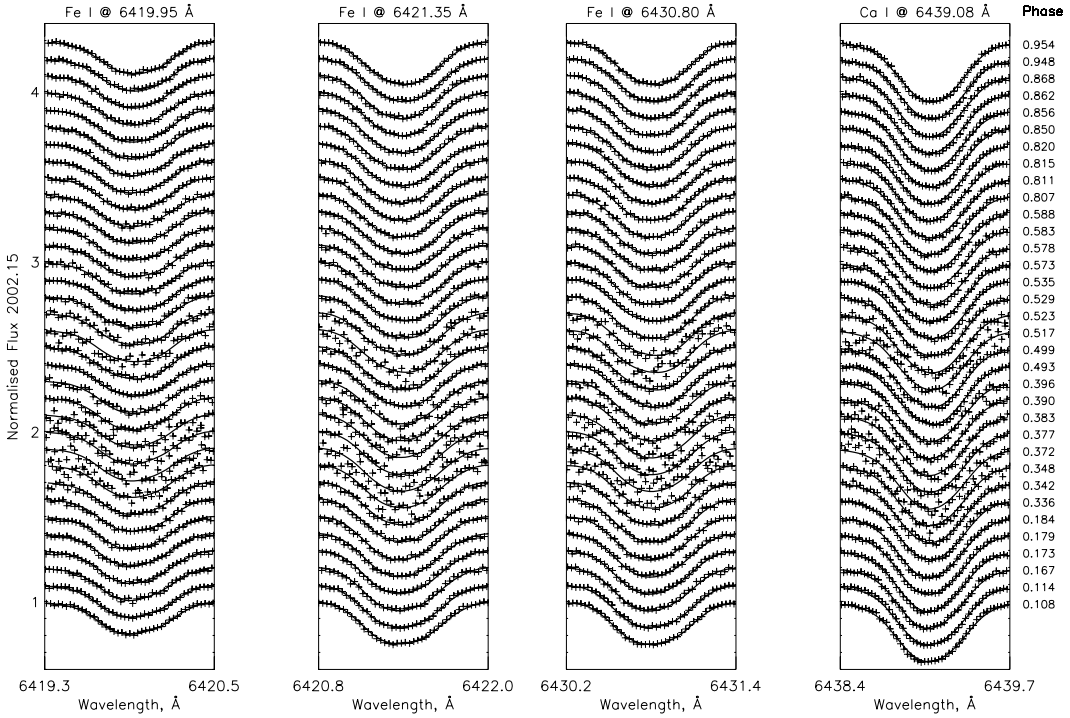

Fig. 7. The same as Fig. 6 for the 2002.16 data set.

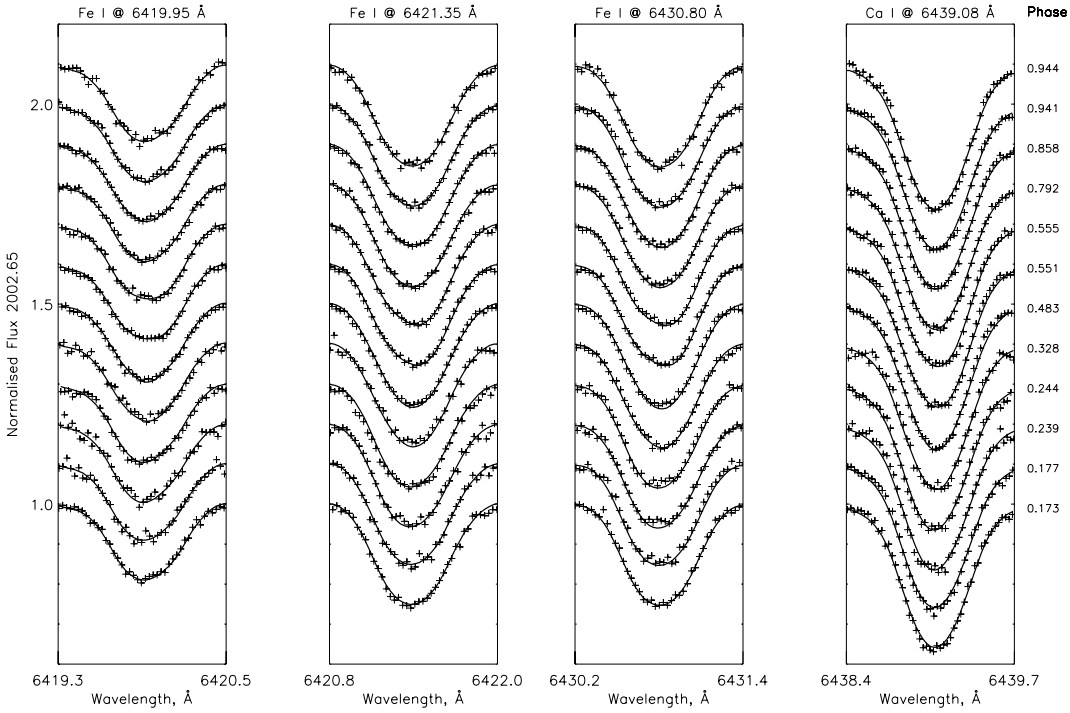

Fig. 8. The same as Fig. 6 for the 2002.65 data set.